

ences between the planar and conical shock-wave detachment angles and behavior become greater as the ratio of specific heats decreases from 1.67 to 1.0<sup>+</sup>. The usually available results for  $\gamma = 1.4$  are not good approximations over the possible range of ratio of specific heats. A complete set of charts, in the format of Ref. 1, is available in Patel et al.<sup>3</sup> for  $\gamma = 1.0^+$ , 1.1, 1.2, 1.3, 1.4, 1.5, 1.6, and 1.67.

### References

- <sup>1</sup>Anon., "Equations, Tables, and Charts for Compressible Flow," NACA TR-1135, 1953.
- <sup>2</sup>Brower, W. B., *Theory, Tables, and Data for Compressible Flow*, Hemisphere, New York, 1990.
- <sup>3</sup>Patel, B. B., Hodge, B. K., and Koenig, K., "Addendum to AIAA Paper 93-0970 Supersonic Axisymmetric Conical Flow Charts for Different Ratios of Specific Heats," Rep. TFD-93-1, Mechanical Engineering Dept., Mississippi State Univ., MS, Jan. 1993.
- <sup>4</sup>Busemann, A., "Drucke auf Kegelformige Spitzen bei Bewegung mit Überschallgeschwindigkeit," *Zeitschrift für Angewandte Mathematik und Mechanik*, Vol. 9, 1929, p. 496.
- <sup>5</sup>Taylor, G. I., and Maccoll, J. W., "The Air Pressure on a Cone Moving at High Speed," *Proceedings of the Royal Society of London, Series A: Mathematical and Physical Sciences*, Vol. 139, 1933, pp. 278-311.
- <sup>6</sup>Anderson, J. D., *Modern Compressible Flow with Historical Perspective*, 2nd ed., McGraw-Hill, New York, 1990.
- <sup>7</sup>Kopal, Z., "Tables of Supersonic Flow Around Cones," Massachusetts Inst. of Technology, Boston, MA, MIT Center of Analysis Rep. TR-1, 1947.
- <sup>8</sup>Sims, J. L., "Tables of Supersonic Flow Around Right Circular Cones at Zero Angle of Attack," NASA SP-3004, 1964.

## Removal of Orbital Debris from Low Earth Orbit by Laser-Generated Drag

Mengu Cho\*

Kobe University, Kobe 657, Japan

### I. Introduction

IN the near future, human space activities will result in significant increases in spacecraft size and the operational time in the orbit. One important issue to be resolved before this new era of the space development is the collision between spacecraft and orbital debris. In low Earth orbit the quantity of man-made orbital debris exceeds the number of natural meteoroids.<sup>1</sup> The pieces of debris that range from 1 to 10 cm are the most threatening because although they are too small to detect from the ground they are too large to shield. In this paper, we propose a method to remove the orbital debris of 1 ~ 10 cm from low Earth orbit. We propose the use of laser pulses to generate drag to the debris; the orbital altitude will be lowered until the debris enters Earth's atmosphere and is burned up because of atmospheric heating.

It has long been known that a giant laser pulse irradiated to solid surface can produce thrust. The concept of using such a thrust for rocket propulsion is not new. Kantrovitz proposed the use of a laser beam to launch a rocket from the ground.<sup>2</sup> The principle of the debris deceleration is the same as the laser rocket propulsion. The pulse of a laser is radiated from a laser satellite to a solid target. Then the target surface is heated by the laser beam, the surface material vaporizes, and plasma is ignited in the vapor that absorbs the laser energy further. The high-temperature gas expands into a vacuum, converting the thermal energy into kinetic energy. The momentum of the hot gas is given to the remaining mass of the debris, just as in usual rocket propulsion.

In the present Note, we first describe the basic specifications of the laser satellite system. Second, we do numerical simulations of

the debris removal to calculate how much laser energy is needed to remove the debris. Third, we discuss our findings.

### II. System Specification

A schematic picture of the laser satellite system is shown in Fig. 1. We propose to put a laser satellite into the Earth-circulating orbit at 700-km altitude. This altitude is chosen because the debris mainly is distributed within a 300-1100 km altitude.<sup>1</sup> The range of a laser beam is assumed to be 500 km, so one satellite can cover the entire area. The satellite power is provided by 25 kW solar arrays. We distribute 20 kW to the laser power supply and 5 kW to other, housekeeping uses, including the telescope operation. Because the satellite cannot always find debris, a battery is used to store the electricity while the laser is not operating. Assuming that the maximum operational rate of the laser is 10%, the laser can use 200 kW on average. For a laser efficiency of 5%, the laser average output is 10 kW.

As the laser source, we choose a 0.25  $\mu\text{m}$  KrF excimer laser, because of its high power output and short wavelength. The laser beam is pointed by a gimbaled telescope. The laser pointing accuracy of 0.1  $\mu\text{rad}$  is assumed, which is technically challenging but not impossible, judging from the state of art of the laser intersatellite communication.<sup>3</sup> As the spot diameter, we assume 0.1 m at 500 km distance. This spot can be made by a mirror of 1.6-m diam at the satellite. The spot diameter at the target is adjusted so that

$$d_{\text{spot}} = 1.27(\lambda R/D_{\text{mirror}}) \quad (1)$$

where  $\lambda = 0.25 \mu\text{m}$ ,  $D_{\text{mirror}} = 1.6 \text{ m}$ , and  $R$  is the distance to the debris. The minimum spot diameter is set at 1 cm because if we focus the laser beam too much, the resulting vapor pressure might exceed the material strength of the target material, thus producing more debris.

To deliver the appropriate momentum to the target, the target surface must be vaporized and plasma must be ignited. Reference (4) shows the momentum change of several materials induced by KrF laser irradiation. The momentum change becomes significant for a laser fluence higher than  $3 \times 10^4 \text{ (J/m}^2\text{)}$ . Below this fluence, the laser intensity is not strong enough to cause the vapor breakdown. Because the spot diameter at 500 km is 0.1 m, we assume 500 J as the laser energy per pulse and 50 ns as the pulse time. Then the laser intensity at the target is  $I_L = 10^{12} \text{ (W/m}^2\text{)}$ . Because the laser can use 200 kW in the operation, the repetition frequency is 20 pps.

We now discuss the pointing and tracking scheme. The debris is first detected by the onboard telescope. The telescope, with 1.6 m aperture diameter can detect debris as small as 1 cm from a 500-km distance by detecting the visible solar reflection with a charge coupled device (CCD) sensor. The field of view of one CCD pixel must be large enough to keep the object within view while it accumulates the electric charges. Therefore, the debris orbit still has a large uncertainty of 10-100  $\mu\text{rad}$ , depending on the field of view of one CCD pixel. Once the debris is detected, the fine pointing is made by laser radar using the KrF laser A in Fig. 1. The probable positions of the debris masses are scanned by the laser pulses, and the light reflection is measured by the UV detector. After the debris orbits are determined within the accuracy of 0.2  $\mu\text{rad}$ , a giant laser pulse is shot from the KrF laser B to generate drag. Once drag is given to

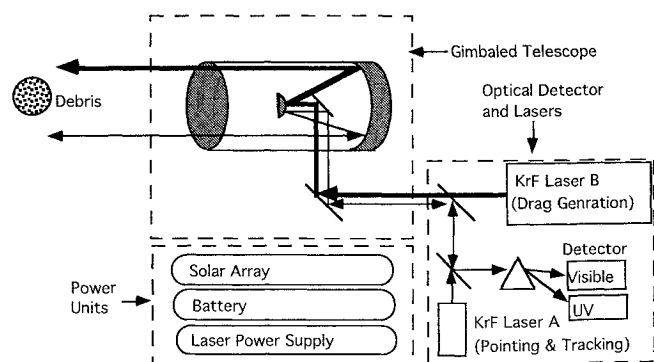


Fig. 1 Schematic picture of debris-removal laser satellite.

Received Jan. 15, 1993; revision received May 14, 1993; accepted for publication July 12, 1993. Copyright ©1994 by the American Institute of Aeronautics and Astronautics, Inc. All rights reserved.

\*Research Associate, Graduate School of Science and Technology. Member AIAA.

the debris, the debris motion departs from the expected path. The correction is made by measuring the reflection of the laser pulses shot from the laser A in Fig. 1.

### III. Simulation

We now simulate the orbital motion of a debris fragment under the laser irradiation. The laser satellite is at the equatorial circular orbit altitude of 700 km. We assume that the debris is initially at a circular orbit with the radius  $r_d$  and the orbital inclination  $i$ . The laser beam is always at the direction  $r_d - r_l$ , where  $r_d$  and  $r_l$  are the position vectors of the debris and the satellite taken from the center of the Earth, respectively. The laser beam is shot only when the tangential velocity of the debris is decelerated. As long as this condition holds and the debris is within the 500-km laser range, the laser pulses are shot toward the debris. The debris velocity  $V$  and the mass  $m_d$  after the  $n$ th laser pulse are given by

$$V^{n+1} = V^n + (C_m J / m_d^n) \hat{e}_t \quad (2)$$

$$m_d^{n+1} = m_d^n - C_v J \quad (3)$$

where  $J$  is the laser energy per pulse,  $J = 500(J)$ , and  $\hat{e}_t$  is the unit vector in the direction of  $r_d - r_l$ . The factor  $\mathfrak{R}$  represents the fraction of the debris cross section within the laser spot area. It is  $\mathfrak{R} = A_{\text{debris}}/A_{\text{spot}}$  when  $A_{\text{debris}} < A_{\text{spot}}$  and unity when  $A_{\text{debris}} \geq A_{\text{spot}}$ . The spot area is given by  $A_{\text{spot}} = \pi d_{\text{spot}}^2/4$  from Eq. 1. We assume that the impulse is generated in the opposite direction of the laser beam because the hot gas expands one-dimensionally, absorbing the laser energy. In Eqs. (2) and (3), we call  $C_m$  and  $C_v$  the momentum and vaporization coupling coefficients, respectively. From Ref. 4, we assume  $C_m = 2 \times 10^{-5} (\text{N} \cdot \text{s}/\text{J})$  and  $C_v = 6.4 \times 10^{-9} (\text{kg}/\text{J})$ . These numbers correspond to a specific impulse of 320 s.

Between the laser pulses, the debris motion is affected by the atmospheric drag and the Earth gravity. The atmospheric density is modeled by the 1976 U.S. Standard Atmosphere. The drag coefficient is assumed to be 1.0 and the cross-sectional area is given by  $A_{\text{debris}} = 1.2(m_d/\rho_d)^{2/3}$ , where  $\rho_d$  is the debris mass density  $\rho_d = 2.7 \times 10^3 (\text{kg}/\text{m}^3)$ . The debris orbit is integrated until the perigee point becomes less than 160 km. Once the perigee point becomes less than 160 km, the atmospheric drag will quickly decelerate the debris, and we do not need the laser to impose the artificial drag. From the 160-km altitude, the decay time to a 100-km altitude is less than one month for debris lighter than 1 kg. For the simulation, we choose  $r_d$ ,  $i$ , and  $m_d$  as the input parameters. The debris and the laser satellite are initially 180 deg apart, except  $r_d = r_l$  where the initial separation is taken to be 2 deg.

In Fig. 2 we show the total laser energies required to remove the debris from the orbit. The laser energies are between  $10^4$  and  $10^8$  J. The right axis of the figure indicates the number of laser shots. For most cases, a few thousand pulses are enough to remove the debris. Because the repetition frequency is 20 pps, the required time is several minutes. When the debris altitude is the same as the satellite, it requires the least laser energy, because the direction of the vector  $r_d - r_l$  becomes the most antiparallel to the debris tangential velocity.

When the debris has a nonzero orbital inclination with respect to the laser satellite, the required laser energy does not differ so much from the zero-orbital inclination case. However, the larger the orbital inclination is, the shorter time the debris is within the laser range. Therefore, for a large orbital inclination, it is likely that we cannot remove the debris during the first encounter. We have to wait until the debris again approaches the satellite. In Fig. 3 we show the time required to remove the debris, changing the orbital inclination as the parameter. The time is measured from the first shot. Although the higher orbital inclination requires the longer time, the time is at most one year.

While one debris mass goes out of the laser range, the laser satellite can work on other debris within the range. The detection rate by the onboard telescope depends on the field of view of the telescope. With the field of view of 0.5 deg and the debris flux of  $10^{-5} (1/\text{m}^2/\text{yr})$ ,<sup>1</sup> in every 500 s one debris fragment can be detected within

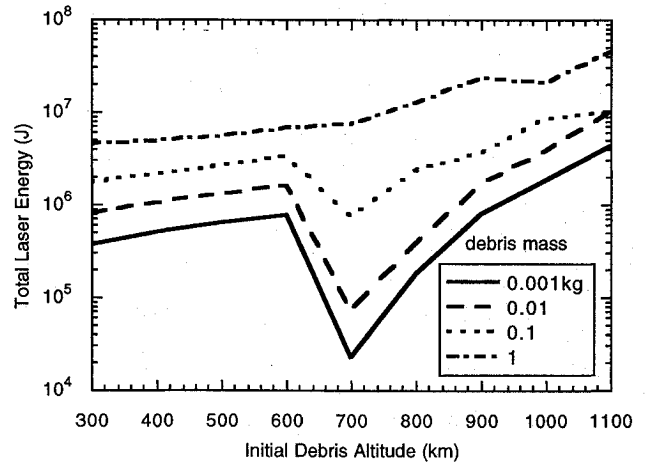


Fig. 2 Laser energy required for debris removal for various initial debris masses and altitudes. The debris orbital inclination is 0 deg.

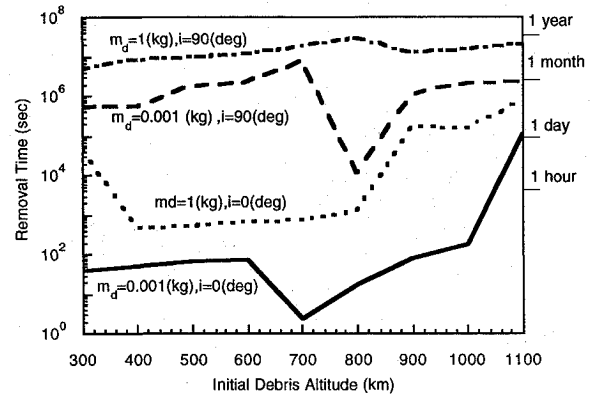


Fig. 3 Time to remove debris for various debris masses and orbital inclinations.

500 km from the laser satellite. If we assume that the satellite spends 1% of the orbital time on debris removal, it can remove 6000 pieces of debris in one year with 1000 shots per debris fragment. Even if the detected debris already is traveling in the direction of the thrust to the tangential velocity imparted by the laser beam, the laser satellite can still use its radar to determine the orbital elements. Therefore, the laser satellite can be used not only to remove the debris but also to catalogue the orbital elements of the debris that are invisible from the ground.

### IV. Discussion and Conclusion

We have seen that laser-generated drag is a very effective way to remove orbital debris from the low Earth orbit. A simplified simulation shows that we require only  $10^4 \sim 10^8$  J to remove the orbital debris of 1 g  $\sim$  1 kg, which corresponds to the length scale 1  $\sim$  10 cm. These objects are lethal to spacecraft but are very hard to track from the Earth. The number of such debris fragments is estimated to be 40,000.<sup>1</sup> With the removal rate of 6000 debris fragments per year, the laser satellite can significantly enhance the safety of the low-Earth-orbit environment. The laser satellite also can be used to catalogue debris invisible from the ground. The catalogued information is used for emergency maneuvering of other spacecraft.

There are many technological issues to be solved before we build this debris removal system. In the present work, we have assumed a KrF laser with 500 J per pulse at 20 pps. The KrF laser with the 500 J output already exists, although the pulse repetition frequency 20 Hz is challenging. A high-powered excimer laser uses a very heavy power supply, and a drastic mass reduction must be made if it is launched into space. Operation of a high-powered laser in space is an undeveloped technological area. The laser system must operate at a maintenance-free condition for many months in the harsh space environment. The optical system must sustain the repetitive irradiance of the high-powered UV light. The low laser efficiency means

that we have to deal with massive residual heat. The high-voltage operation in space also causes an insulation problem of the satellite surface under the ionospheric plasma environment.

One big problem would be the pointing and tracking of the debris. We have assumed a pointing accuracy of  $0.1 \mu\text{rad}$  with a 1.6-m telescope. Accurately tracking a fast-moving object with such a large telescope is very challenging. In the numerical simulations in Sec. III, the steering speed required for the gimbaled telescope is calculated to be  $\omega = 4.3(\text{deg/s})$  and  $\dot{\omega} = 8.6(\text{deg/s}^2)$  for debris at an altitude of 800 km and with 90 deg inclination. This laser satellite system has many elements in common with laser intersatellite communication, for which several space experiments are planned in the near future. With minor modifications to the experimental equipment, the debris pointing and tracking experiment can be conducted on the same platform. Because the proposed laser satellite is gigantic, this approach is a reasonable first step.

### Acknowledgments

The author thanks Prof. Kaya of Kobe University, Prof. Sato of Kyoto University, Prof. Takano, and Mr. Tanaka of ISAS, Dr. Fujise and Mr. Inagaki of ATR, Mr. Arimoto and Mr. Suzuki of CRL, and Prof. Ueda of Telecommunications University for their valuable comments and criticisms.

### References

- <sup>1</sup>Griffin, M. D., and French, J. R., *Space Vehicle Design*, Education Series AIAA, Washington, DC, 1991, Chap. 3.
- <sup>2</sup>Kantrovitz, A., "The Relevance of Space," *Astronautics and Aeronautics*, Vol. 9, No. 3, 1971, pp. 34-35.
- <sup>3</sup>Bailly, M., and Perez, E., "The Pointing, Acquisition, and Tracking System of SILEX European Program: A Major Technological Step for Intersatellites Optical Communication," *SPIE Optical Engineering Reports*, Vol. 1417, 1991, pp. 142-157.
- <sup>4</sup>"Report to the American Physical Society of the Study Group on Science and Technology of Directed Energy Weapons," *Reviews of Modern Physics*, Vol. 59, No. 3, 1987, pp. S1-S201.

## Calculating the Number of Meteoroid Impacts onto a Gravity-Gradient-Stabilized Spacecraft

Michael D. Bjorkman\*  
Boeing Defense & Space Group,  
Huntsville, Alabama 35824-6402

### Introduction

THE meteoroid shield assessment procedure<sup>1</sup> developed for Apollo implicitly assumes a randomly tumbling spacecraft stationary with respect to the meteoroid environment measured by Earth-based sensors, i.e., a spacecraft with no orbital speed. In order to determine the effect of this assumption on the reduction of spacecraft-borne meteoroid sensor data and on spacecraft meteoroid shield assessment, Kessler<sup>2</sup> performed an analysis showing that the spacecraft orbital speed results in negligible increase of the calculated flux onto a randomly tumbling spacecraft. Hence, most analysts have not included the effect of spacecraft speed in their analyses.

With the approaching retrieval of the gravity-gradient-stabilized spacecraft LDEF, Zook<sup>3</sup> reexamined the effect of spacecraft speed on the meteoroid flux onto a spacecraft. He showed that even though there is only a small increase in number of impacts onto the vehicle

as a whole, the number of impacts onto the fore portions of the spacecraft is an order of magnitude larger than onto the aft. Thus the effect of spacecraft speed is crucial to understanding the distribution of impacts around a gravity-gradient-stabilized spacecraft such as LDEF and the Space Station.

Two assessment procedures for gravity-gradient-stabilized spacecraft have been published. Sullivan and McDonnell<sup>4</sup> specialized their procedure to the case of a meteoroid environment with a single speed. Zook,<sup>3</sup> using a procedure similar to that suggested by Kessler,<sup>2</sup> made a more realistic calculation by starting from the measured meteor closing-speed probability density function. First he calculated small increments of the mean number of impacts on a spacecraft with velocity  $v_s$  in the stationary spacecraft reference frame for small increments of meteoroid closing speed  $v$  and polar approach angle  $\psi$ . Second, he transformed the coordinate increments from the stationary spacecraft reference frame to coordinate increments in the orbiting spacecraft reference frame, in which the spacecraft is at rest. Last, he sorted the increment of the mean number of impacts into the appropriate orbiting spacecraft coordinate bins, where a running sum for the mean number of impacts was kept for each bin.

An alternative to Zook's numerical procedure is described here. Because the meteoroid environment may be described in terms of continuous probability density functions, it is possible to use a Jacobian to describe the coordinate transformation and the integral calculus to calculate the mean number of impacts. The results from this approach are compared with Zook's calculation of the ratio of the fluxes on the fore and aft facing sides of a flat plate.

### Meteoroid State

The state of the meteoroid is defined as its closing speed and its approach angle with respect to the reference surface that registers the impacting meteoroid flux. Thus, the meteoroid state is a function of the shape of the reference surface and the velocity of the reference surface relative to the meteoroid environment. A complete description of the meteoroid state is only available for meteors. Kessler<sup>2</sup> has shown that the approach angles of meteoroids entering the Earth's atmosphere are isotropically distributed with respect to the Earth, and consequently the meteoroid closing speed is independent of approach angle. (Note that any point on the surface of the Earth may not see an isotropic distribution of approach angles, but the Earth's surface as a whole will.) Thus the probability of a meteoroid having a certain state with respect to the Earth is the product of the isotropic approach-angle probability density function with the closing-speed probability density function.

This closing-speed probability density function  $g(v)$  was measured for photographic meteors by Hawkins and Southworth.<sup>5</sup> These data were later analyzed by Erickson<sup>6</sup> to eliminate observational selection effects, and the resulting graphical closing-speed probability density function was fitted by Zook<sup>7</sup> with the equations

$$g(v) = \begin{cases} 0.1120, & 11.1 \text{ km/s} \leq v \leq 16.3 \text{ km/s} \\ 3.328 \times 10^5 v^{-5.34}, & 16.3 \text{ km/s} \leq v \leq 55.0 \text{ km/s} \\ 1.695 \times 10^{-5}, & 55.0 \text{ km/s} \leq v \leq 72.2 \text{ km/s} \end{cases} \quad (1)$$

To make the connection with spacecraft, note that a randomly tumbling flat plate will also see an isotropic distribution of approach angles. Therefore, the function  $g(v)$  can be thought of as the closing-speed probability density function for an imaginary randomly tumbling flat plate stationary with respect to the Earth, with  $v$  the meteoroid closing speed measured relative to the randomly tumbling flat plate.

Surprisingly, the meteoroid state description for meteoroids striking a fictitious stationary randomly tumbling flat plate can be used to make acceptable estimates of the flux onto an orbiting randomly tumbling flat plate. Kessler<sup>2</sup> has shown the ratio of the flux on an orbiting randomly tumbling flat plate to the flux on a stationary randomly tumbling flat plate is

$$1 + v_s^2 \int_{v_{\min}}^{v_{\max}} \frac{g(v)}{v^2} dv \quad (2)$$

Received Jan. 9, 1994; revision received March 25, 1994; accepted for publication June 8, 1994. Copyright © 1994 by Michael D. Bjorkman. Published by the American Institute of Aeronautics and Astronautics, Inc., with permission.

\*Principal Engineer, P.O. Box 240002, M/S JR-34.